at current densities of about 40 A/cm², which is within the state of the art, with a microperveance of 1.4 (which is comparable to the microperveance of the SLAC tubes shown in Table 9.3). The design voltage is 600 kV, and the total current is 6.7 kA, with a projected pulse length of 1 μsec and repetition rate of 10 Hz. The beams pass through four common stagger-tuned cavities, as well as an individual second-harmonic cavity for each beam to enhance bunching. Internal feedback and a gain of 30 dB would allow the tube to oscillate at a frequency of 1.5 GHz without a separate driving source. PPM focusing is used for each beam line separately. With a design output power of 2 GW, the efficiency is to be 50%; fields of 200 kV/cm in the output cavity are comparable to those in previous SLAC klystrons. Although the project was terminated before the tube was constructed, it was to have a length of about 1.5 m and a mass of about 82 kg, both parameters stated without including the power supply and auxiliary equipment such as cathode heaters and vacuum pumps.

The GMBK is one direction of possible development for conventional (SLAC) klystron development aimed at genuine HPM performance. The sheet-beam klystron is another suggested direction for development aimed at producing a simpler, lower-cost alternative to SLAC klystrons operating around 100 MW. The sheet-beam klystron employs a planar, strip-like electron beam, much wider in one cross-sectional dimension than the other. Although first proposed in the Soviet Union in the late 1930s, and despite the advantages its large lateral dimensions offer in terms of reduced cathode current density and lower power density in the cavities, sheet-beam klystron operation is complicated by the need for large drift tubes and overmoded cavities and by the attendant questions about beam transport. Further, the design of a sheet-beam electron gun promises to be a demanding engineering challenge, and to date, none have been built for this application. Nevertheless, the cost-driven requirement of the Next Linear Collider for a 150-MW peak, 50-kW average, 11.4-GHz klystron was regarded as potentially too demanding for a pencil-beam klystron with a 1-cm bore in the drift tube, which led to the recommendation for the double sheet-beam klystron shown in Figure 9.32.[57] This device features two sheet-beam klystrons operated side by side, each generating 75 MW of X-band radiation for a total of 150 MW, assuming roughly 50% power efficiency. Each klystron in this pair has an input cavity followed by two gain cavities, a penultimate cavity, and an output cavity. In this design concept, the beams from 450-kV, 320-A electron guns with a cathode current density of 5 A/cm² are magnetically compressed to a current density of 50 A/cm². The beam cross-sectional dimensions are 0.8×8 cm², and the drift tube has a height of 1.2 cm. The input, gain, and penultimate cavities are so-called triplets, consisting of three closely coupled cavities, as one can see in Figure 9.32, a cavity design that solved the problem of inadequate cavity coupling for a singlet cavity. The output cavity, on the other hand, has five of these cavities, and output from each beam and output cavity is coupled out through its own window. Calculations indicate a cavity isolation of 50 dB over 5 cm, and MAGIC simulations point to a 68-dB overall

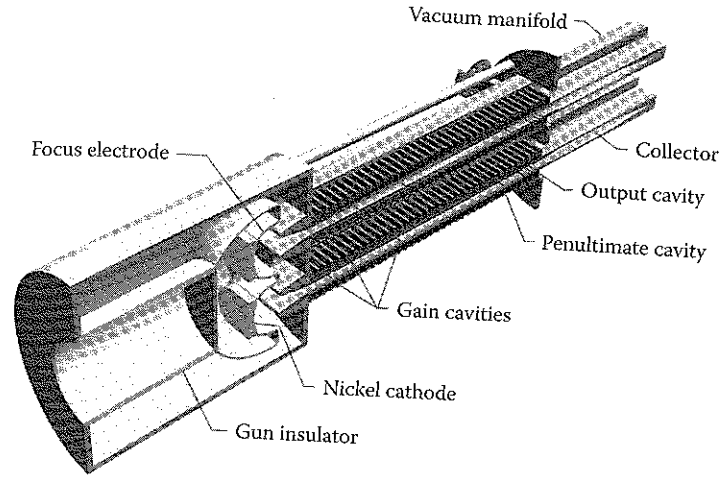

FIGURE 9.32
Cutaway schematic drawing of the double sheet-beam klystron. (Courtesy of George Caryotakis, SLAC.)

tube gain. Although the gun design issues were not yet fully addressed, the suggested performance, the greater simplicity of the device relative to a multibeam klystron, and the technical risk associated with a pencil-beam, 150-MW klystron argued in favor of building a SBK or double SBK for further experimental investigation.

9.5.2 Low-Impedance Annular-Beam Klystrons

Following the first two phases of development for low-impedance, annular-beam klystrons, the NRL group proposed a major design modification, the triaxial klystron with an annular electron beam propagating through a drift space bounded by both inner and outer cylindrical walls (see Problem 24).[47] The schematic layout of an experimental version is shown in Figure 9.33.[58] This configuration has two major advantages over the coaxial version. First, provided the transverse electromagnetic modes are suppressed — and they did not pose a problem in the experiments — this geometry can support large-radius electron beams as long as the distance between the inner and outer conductors is limited to about half of the vacuum wavelength of the microwaves produced. Second, the space-charge-limiting current for this geometry is, in principle, about twice that of the coaxial geometry, which we can see from the expression for the space-charge-limiting current for a thin annular beam, which is of the general form

$$I_{SCL} = I_s\left(\gamma_0^{2/3} - 1\right)^{3/2} \tag{9.35}$$

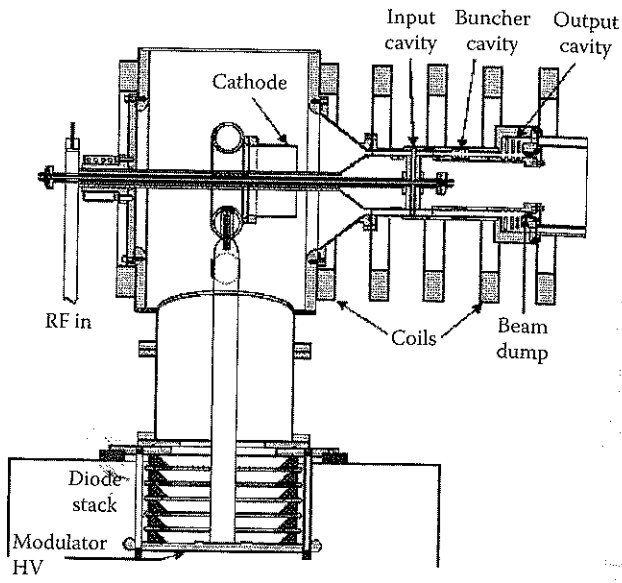

FIGURE 9.33
Layout of an experimental version of the triaxial klystron. (From Pasour, J. et al., *High Energy Density and High Power RF, 6th Workshop*, Berkeley Springs, WV, 2003, p. 141. With permission.)

The expression for I_s is given by Equation 9.3a for a coaxial klystron with beam radius r_b and drift tube radius of r_0; in a triaxial klystron with inner and outer drift tube radii of r_i and r_o, however,

$$I_s = 8.5\left[\frac{1}{\ell n\left(r_o / r_b\right)} + \frac{1}{\ell n\left(r_b / r_i\right)}\right] \text{ kA} \tag{9.36}$$

(see Problem 9.27). On a practical basis, though, if beam transport requirements limit the beam–wall standoff to a distance Δ that is approximately independent of beam radius, then

$$I_{SCL} \approx 8.5\left(\frac{2r_b}{\Delta}\right)\left(\gamma_0^{2/3} - 1\right)^{3/2} \text{ kA} \tag{9.37}$$

This expression shows that the freedom to build large-radius triaxial klystrons while maintaining the cutoff condition between cavities provides an open-ended scaling with radius of the current-carrying capacity of the device. Two additional advantages of the triaxial device are (1) that a lower magnetic field can be used for beam confinement, in a geometry that would allow permanent magnets to be used, and (2) the inner conductor helps stabilize streaming and velocity–shear instabilities of the electron beam.

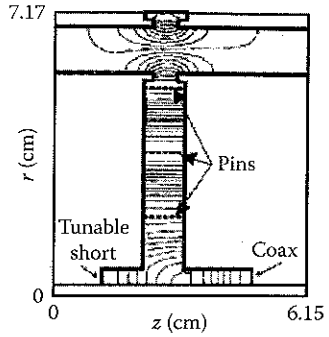

FIGURE 9.34
Input cavity of the experimental triaxial klystron of Figure 9.33. The field pattern was calculated with SUPERFISH. (From Pasour, J. et al., *High Energy Density and High Power RF, 6th Workshop*, Berkeley Springs, WV, 2003, p. 141. With permission.)

Returning to the experimental layout of Figure 9.33, we see first that the negative voltage pulse is fed to a corona ring to which the cylindrical cathode is attached. This configuration allows RF feed to the first cavity, as well as the support for the grounded inner conductor, to pass through the cathode ring and cylinder. The cathode emitter is CsI-coated graphite fiber, which produces a 4-kA beam at 400 kV, for a beam impedance of 100 Ω. The cathode radius is 7.2 cm; a slightly converging magnetic field of 0.2 to 0.3 T reduces the beam radius to r_b = 6.25 cm, at which it was optimized for microwave generation in the downstream cavities. The beam dump at the far end of the drift tube is a tapered graphite ring between the inner and outer conductors.

The signal is fed through a coax to a radial input cavity with a radius chosen to be an odd number of quarter wavelengths in order to maximize the axial component of the electric field at the beam radius. The cavity and a SUPERFISH calculation of the field lines are shown in Figure 9.34. For the 9.3-GHz frequency of the experimental klystron, the cavity extended (7/4)λ in the radial direction; the field structure was reinforced by placing thin conducting pins at the expected location of the field nulls. These pins also provide additional mechanical support for the inner conductor as well as a return path for the beam current along the inner conductor. The bunching cavity downstream of the input cavity is a five-gap standing wave structure operating in the π-mode with a cavity spacing of 1.3 cm and a depth of a quarter wavelength, measured from the axis of the drift tube to the cavity wall. The field pattern for this structure is shown in Figure 9.35. A four-gap version of the output cavity is shown in Figure 9.36a. The gaps in the outer wall extract microwave power into a coaxial line; the gap spacing is tapered to maintain synchronism with the beam electrons as they lose energy and slow down. Slots cut into the inner wall match the gaps in the outer wall. Conducting pins in the outer gaps reinforce the desired field pattern there and also provide added mechanical strength for the structure. SUPERFISH calculations were used to establish the basic field

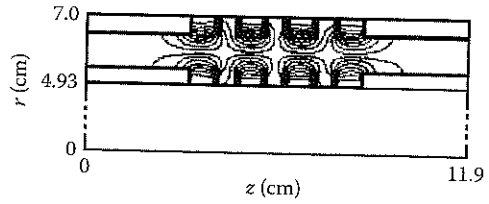

FIGURE 9.35
Five-gap standing wave bunching cavity for the experimental triaxial klystron of Figure 9.33. (From Pasour, J. et al., *High Energy Density and High Power RF, 6th Workshop*, Berkeley Springs, WV, 2003, p. 141. With permission.)

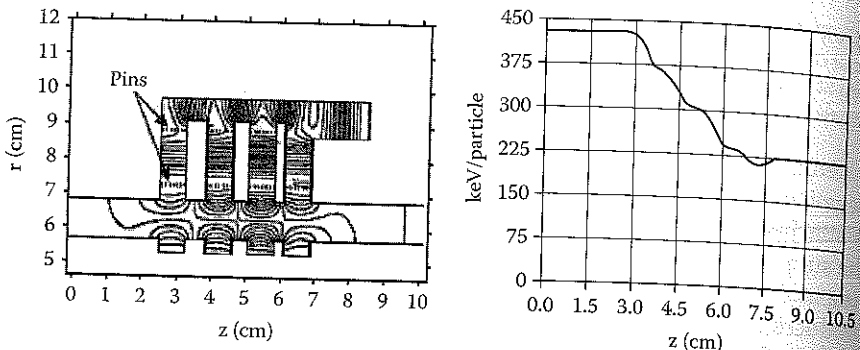

FIGURE 9.36
(a) Geometry of the output cavity used in a MAGIC simulation of the triaxial klystron of Figure 9.33. (b) Energy loss of electrons from a 440-kV, 5-kA beam with 75% current modulation, computed with MAGIC. (From Pasour, J. et al., *High Energy Density and High Power RF, 6th Workshop*, Berkeley Springs, WV, 2003, p. 141. With permission.)

structure in the output cavity, then MAGIC particle-in-cell simulations were employed to optimize the energy extraction efficiency from a prebunched beam assumed to have 75% current modulation, based on simulations of the upstream beam dynamics. MAGIC results indicated 50% energy extraction from a 440-kV, 5-kA beam, for a calculated output of 1.1 GW. The computed loss of electron energy in the output cavity is illustrated in Figure 9.36b, which shows that the bulk of the energy is lost in the first three gaps. The peak electric field of about 400 kV in the output gaps is about half of the Kilpatrick breakdown field.

In actual experiments, a commercial 250-kW pulsed magnetron provided the input signal. Current modulation from the first cavity reached a maximum about 10 cm downstream. An output power of about 300 MW was reached, for a gain of just above 30 dB. For a 420-kV, 3.5-kA electron beam, the efficiency was about 20%. Increasing the beam power also increased the output microwave power, but at the expense of pulse shortening by erosion at the tail end of the microwave pulse. Decreasing the magnetic field somewhat appeared to increase the pulse length, suggesting that multipactoring might be occurring in the output cavity. Multipactoring in the input cavity was a problem that was solved by polishing the cavity surfaces and reducing the sharpness of the cavity edges. In future experiments, multipactoring was expected to be reduced further by the use of polished copper cavity walls, rather than bronze and brass; improved vacuum; and better isolation of the beam dump. It was also expected that a redesign of the structure to allow better field penetration by the pulsed magnetic field, or even the adoption of permanent magnet focusing, would reduce beam interception by the walls, increasing efficiency further.

This set of experiments clearly demonstrated the desirable features of the triaxial klystron for high-frequency operation in the X-band. The triaxial geometry allowed the use of a beam with a radius almost as large as that of the L-band coaxial system (see Table 9.6). The impedance of roughly 100 Ω is comparable to that of the S-band coaxial klystron in Table 9.6, but at three times that of the L-band klystron, the X-band triaxial klystron does not have the beam power to produce multigigawatt output. Nor, in this initial set of experiments, does it have the necessary efficiency. Although the authors were concerned about the magnetic field penetration in the structure and the resulting effect on beam transport through the device, it was also not clear if the multigap bunching cavity produced the necessary total gap voltage to take advantage of the unique bunching mechanism described by Equations 9.17 and 9.18. Nevertheless, multigap cavities reduce the field stresses that can lead to breakdown.

The slight pulse shortening observed in this device is much less pronounced than that seen in the coaxial klystrons. When Friedman's NRL team raised the output power of their coaxial klystron to 15 GW, the output pulse was shortened to about 50 nsec, with dubious reproducibility. Repeatable power levels of about 6 GW in 100-nsec pulses were achieved. This problem of pulse shortening appears to be common to all high power microwave devices. As we have discussed, many of the problems in low-impedance, annular-beam klystrons have been identified. The triaxial configuration, which allows lower-impedance operation, solves some of these problems by reducing the required operating voltage to achieve a given power, thus reducing the voltage stresses that can create breakdown conditions at a number of locations, while also reducing both the generation of x-rays in the beam collector and the linear, circumferential current density of the beam, which eases beam transport problems. The foregoing tend to erode the microwave pulse from the back. Beam loading of the gap, on the other hand, tends to erode the head of the pulse; this problem was addressed with the use of large gaps. Multigap cavities may address the problem as well, although achieving adequate gain with such cavities may require additional cavities. The need for better vacuum has been recognized, although to date a system operating at higher vacuum has not been explored.

9.6 Fundamental Limitations

The maximum power output that can be obtained from a klystron is the smaller of two limits: that available from the beam and that determined by the breakdown strength at a number of points in the device. The former is expressed in terms of the efficiency, η, and the beam power:

$$P_{out} = \eta V_0 I_b \tag{9.38}$$

Here, we use the anode–cathode voltage in the electron beam diode, V_0, and the electron beam current, I_b. The power efficiency for both high- and low-impedance klystrons has reached about 50%. We can expect that this is practically about the limit for high power klystrons, although, as we discussed in the case of high-impedance klystrons employing PPM focusing, overall system efficiencies can be improved somewhat with the use of permanent magnets, which draw no electrical power, in comparison with pulsed or superconducting electromagnets.

For several reasons, it is more desirable to increase the current rather than the voltage in Equation 9.38. According to the simplified model underlying Equation 9.11, lower voltages correspond to shorter bunching lengths, which reduces device length. We also know that lower voltages reduce both the size of the pulsed power and the chances for breakdown there. Finally, reducing the voltage limits the generation of x-rays in the beam collector, as well as those generated by beam interception within the klystron circuit.

9.6.1 Pencil-Beam Klystrons

The scaling of current with voltage and the terms in which that scaling is expressed vary with both voltage and the preferences of the research communities associated with different device technologies. At nonrelativistic voltages below about 500 kV, and even at voltages somewhat higher in the community associated with high-impedance, pencil-beam klystrons, it is common to express the current in terms of the perveance, K: $I_b = K V_0^{3/2}$. Thus, we can rewrite Equation 9.38:

$$P_{out} = \eta K V_0^{5/2}, \; V_0 < 500 \text{ kV} \tag{9.39}$$

In the case of the high-impedance and low-perveance pencil-beam klystrons, experimental data from Thomson CSF (now Thales) klystrons shown in Figure 9.37 indicate that the efficiency declines as the perveance grows[59]; however, the reference shows that the efficiency can be recovered by adding more bunching cavities, at the cost of added length and complexity.

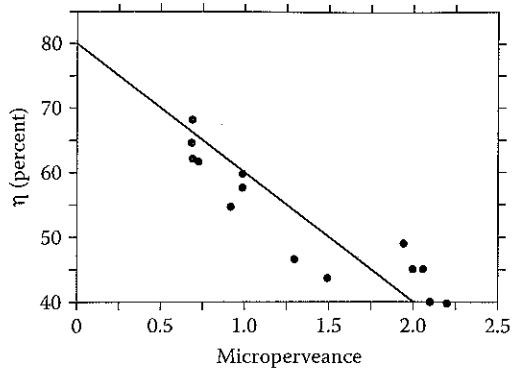

FIGURE 9.37
Reduction of the efficiency with increasing perveance in low-impedance, pencil-beam klystrons. (From Palmer, R. et al., *Part. Accel.*, 30, 197, 1990. With permission.)

Two approaches to increasing the power of this class of klystron were discussed in Section 9.5.1: multibeam and sheet-beam klystrons. The former currently represents the lower-risk approach, both because there is greater experience with multibeam klystrons at lower voltage and power and because even sheet-beam devices would probably have to use multiple beams to approach gigawatt-level performance. The two left columns of Table 9.8 contain a comparison of the 150-MW, S-band SLAC klystron produced for DESY and the proposed multibeam gigawatt klystron (MBGK). Both operate at comparable voltages, and the perveance per beam in the MBGK is actually somewhat lower than that in the lower-power device. By using 10 individual beams, though, the total current in the MBGK is actually about 10 times higher, and the output power, assuming that 50% efficiency can be achieved, is about 7 times that in the single-beam S-band klystron.

TABLE 9.8
Comparison of SLAC Klystron and NRL/RKA and the Enhanced Current Versions Proposed for Each, the GMBK and Triaxial RKA, Respectively

	SLAC/DESY S-Band	GMBK (proposed)	RKA	Triaxial RKA (proposed)
Frequency, GHz	2.998	1.5	1.3	1.3
Beam voltage, kV	525	600	1,000	700
Beam current, A	704	6700	30,000	100,000
Beam microperveance, μA/V$^{3/2}$	1.85	1.4[a]	30	171
Beam impedance, Ω	746	90	33	7
Axial magnetic field, T	0.20		1.0	
Peak output power, GW	0.15	2.0	15.0	
Saturated gain	~55 dB	36 dB		
Efficiency	~50%	50%	~50%	

[a] Per beam, for each of 10 beams.

Obviously, employing multiple beams brings its own complexity to devices of this type, although this technology base will continue to grow at lower power levels, since multibeam klystrons are currently a front-runner for the new S-band superconducting approach for high-energy electron positron colliders.[60]

9.6.2 Annular-Beam Klystrons

In the case of low-impedance, annular-beam klystrons, which operate at voltages of about 500 kV and up, the impedance Z is more appropriate and more commonly used, $I_b = V_0/Z$; now

$$P_{out} = \eta \frac{V_0^2}{Z}, \; V_0 \geq 500 \text{ kV} \tag{9.40}$$

Once again, to achieve high power while limiting the voltage, one wants to operate at low impedance. The right two columns of Table 9.8 illustrate the parameters for both the 15-GW coaxial klystron and a proposed high power triaxial device. These two klystrons differ from the pencil-beam devices in two important ways: the beams are generated with explosive emission cathodes, and the annular beam is topologically more similar to a planar sheet, rather than pencil, beam. The same issues of efficiency vs. perveance therefore do not apply, and we can see that the perveances for annular-beam klystrons are much higher.

Producing high power with an annular-beam klystron while simultaneously controlling the processes that contribute to pulse shortening will require one to address the limitations of these devices in five areas. First, one must provide the requisite current at a manageable voltage, preferably at or below a megavolt. Theoretically, the triaxial configuration has twice the limiting current of the coaxial device, although, as we discussed earlier, the practical current limit for the triaxial geometry is much larger still, given the requirement for a certain beam standoff distance from the wall of the drift tube. Explosive emission diodes can produce the requisite current, albeit at the expense of their well-known problems with gap closure. A thermionic gun operating at 400 Ω (300 kV, 750 A), with a cathode loading of 8 to 10 A/cm^2, has been considered for further experiments with a triaxial klystron,[58] although operation at this higher impedance negates the advantage these devices have in current-carrying capacity in order to ensure more stable repetitive operation.

Second, having generated the beam, one must properly align the beam and the magnetic field within the drift tube, and the magnetic field must be quite uniform along the drift tube as well. These issues were discussed in Friedman et al.[51] Poor alignment can cause beam electrons to be lost to the walls, which in turn causes outgassing, compromising vacuum quality in the device. Similarly, the beam collector must be isolated to prevent contaminating the drift region with impurities released there; one must also address the issue of x-ray generation in the collector.

Third, one must address the issues of cavity design. In the second phase of annular-beam klystron development, capacitive loading in the bunching cavity — which erodes pulses from the leading edge — and potential energy recovery in the extraction region were addressed at gigawatt levels in coaxial devices. In addition, practical matters of cavity wall materials and radiusing of sharp gap edges were found to increase pulse lengths by preventing erosion from the trailing edge of the pulse. In the set of experiments performed with a triaxial klystron, multigap standing wave cavities were employed to distribute the power and reduce the electric fields. This raises the issue of whether a cavity of this type will generate the unique bunching mechanism described by Equations 9.16 through 9.18. If not, this might well raise a fourth issue: achieving adequate gain in these amplifiers. The lower the gain, the higher the required input power to achieve a given output power, and gains of 30 dB in these devices (as opposed to the gains of 50 to 60 dB in pencil-beam klystrons) would require more input power than commercial microwave sources could supply. The issue was raised somewhat in passing in the experimental paper on the triaxial klystron: it may be necessary to use more than one intermediate bunching cavity to raise the gain if one were to desire tens of gigawatts in a large device maximized for power production.

The fifth issue is one that has been appreciated for some time, but one that has not been fully explored in annular-beam klystrons: improving the vacuum levels from typical values of about 10^{-5} torr. This engineering matter involves the use of ceramic, as opposed to plastic, insulators; different vacuum-pumping technology; and greater attention to system cleanliness, perhaps even involving *in situ* discharge cleaning. The improvements to be gained by lowering the vacuum levels remain to be fully explored in these devices.

One issue that has not been addressed in these devices is tunability. The three-cavity structure — input cavity, bunching cavity, and output structure — limits the opportunities for stagger tuning, as one would in conventional or high power, high-impedance klystrons. Mechanical tuning of the cavities, or the addition of cavities if higher gain or stagger tuning is desired, is a possibility if the intrinsic bandwidth is found to be too narrow for some applications.

9.6.3 Reltrons

Reltrons to date have been compact workhorse tubes capable of producing hundreds of megawatts of output for a very broad range of frequencies, made possible by changing out key parts to achieve large frequency jumps, while using mechanical tuning for finer frequency adjustment within different frequency bands. In this power range, either no magnetic field is required or, at the higher power levels requiring higher beam currents, permanent magnets have been adequate. At lower repetition rates, of the order of 10 Hz, velvet cathodes have been employed. If higher power is required, up to

1 GW or beyond, higher current and voltage in the injector may create the need for a guiding magnetic field. Certainly higher repetition rates will demand metallic explosive emission cathodes (outgassing from the velvet limits repetition rates) or perhaps thermionic emitting cathodes.

9.7 Summary

High power klystrons and reltrons are among the most mature of all HPM sources. The extension of the conventional klystron into the relativistic domain resulted in the production of a 200-MW S-band klystron. More significantly, though, an X-band 75-MW klystron was designed to use periodic permanent magnet focusing of the electron beam, a technological advance that eliminates the power consumption of pulsed or superconducting electromagnets. The next steps in development for these tubes, either a sheet-beam klystron to simplify device design and construction costs or a multibeam klystron to achieve gigawatt-level operation, are stalled, the former because of a decision in 2004 to base the future International Linear Collider on a different technology path, and the latter because of lack of sponsorship at this time for this approach to high power klystrons.

Low-impedance, annular-beam klystrons have progressed through the development of annular-beam devices capable of something more than 10 GW of output in the L-band to a new stage of development based on a proposed triaxial geometry that promises higher-current operation with higher output power, as well as better device scaling to higher frequencies. In addition, this geometry may be amenable to the use of periodic permanent magnet beam focusing. The first experiments have been performed with this new configuration. Device performance is rather well understood below several gigawatts of output power, although pulse shortening is an increasingly troublesome issue as power increases above that, and the realm above 10 GW remains largely uncharted territory.

Problems

1. For an anode–cathode accelerating voltage $V_0 = 1$ MV, drift tube radius $r_0 = 5$ cm, and beam radius $r_b = 4$ cm for a thin annular beam, plot the beam current I_b vs. the relativistic factor for an electron, γ_b.
2. The curve of I_b vs. γ_b has a maximum, which is the maximum current that can be propagated through the drift tube for a given accelerating voltage V_0 and beam radius r_b, assuming a thin annular beam. Derive an expression for the maximum current, which is known as the space-charge-limited current, I_{SCL}, as a function of the drift tube radius, r_0, r_b, and the factor $\gamma_0 = 1 + eV_0/mc^2$.
3. Compute the space-charge-limited current I_{SCL} (see Problem 2) for $V_0 = 1$ MV, $r_0 = 5$ cm, and
   a. $r_b = 3$ cm
   b. $r_b = 4$ cm
4. For each value of $I_b < I_{SCL}$, Equation 9.2 yields two values of γ_b. Which value of γ_b — the larger or the smaller — is the physically significant solution to Equation 9.2 (i.e., the real one)? Explain your choice.
5. For $V_0 = 0.8$ MV, $r_0 = 5$ cm, and $r_b = 4$cm, compute γ_b and β_b for a beam electron.
6. For $I_b > 0$, $\gamma_b < \gamma_0$. In fact, γ_b decreases as r_b decreases. Where is the "lost" kinetic energy when the kinetic energy of an electron is $(\gamma_b - 1)mc^2 < eV_0$?
7. What magnetic field is required to confine a pencil beam of current $I_b = 400$ A and radius $r_b = 2$ cm that was generated by a 500-kV electron gun? For convenience, assume $\gamma_b = \gamma_0$.
8. Which mode has the lowest cutoff frequency in a cylindrical drift tube (which, of course, acts as a waveguide)? Which mode has the second-lowest cutoff frequency in a cylindrical waveguide?
9. In a cylindrical waveguide, what is the maximum radius at which waves of the following frequencies are cut off?
   a. 1 GHz
   b. 3 GHz
   c. 5 GHz
   d. 10 GHz
10. In the absence of a beam, purely electromagnetic waves propagate in a cylindrical waveguide according to the dispersion relation

$$\omega^2 = \omega_{co}^2 + k_z^2 c^2$$

where $\omega = 2\pi f$ and $k_z = 2\pi/\lambda$, with λ the wavelength along the waveguide axis. Let $f = 1.3$ GHz. Suppose that over a distance of 10 cm, you want a 1.3-GHz electromagnetic wave to be attenuated by at least 30 dB. Assuming that the waveguide walls are perfectly conducting (i.e., ignoring resistive losses in the wall), what must the waveguide radius r_0 be to ensure at least that level of attenuation?

11. Assuming that the gap capacitance C of a coaxial cavity of characteristic impedance Z_0 is small (i.e., $Z_0\omega C << 1$), estimate the three smallest values of the allowable lengths of the cavity at the following frequencies:

a. 1 GHz
b. 3 GHz
c. 5 GHz
d. 10 GHz

12. The modulation factor M for a planar beam transiting a thin gap is given by Equation 9.9. Compute M for a gap of width 5 cm and the following parameter values, assuming $\gamma_b = \gamma_0$:
    a. $V_0 = 200$ kV, f = 1.3 GHz
    b. $V_0 = 500$ kV, f = 1.3 GHz
    c. $V_0 = 500$ kV, f = 3 GHz
    d. $V_0 = 500$ kV, f = 10 GHz
13. Derive the expression for the modulation factor M in Equation 9.9 for a beam of large cross section transiting a gap of width g between two parallel plates with a time-varying voltage $V = V_1 e^{-i\omega t} = -Ege^{-i\omega t}$ applied across the gap. Assume the field does not vary with distance across the gap and that the change in the electron velocity due to the modulation is much smaller than the velocity of the electrons entering the gap, v_b.
14. Developers of the low-impedance relativistic klystron found that large gaps could be used to mitigate beam-loading effects on the cavities that were eroding the leading edge of the microwave pulse. The gaps were so large that the sign of the electric field reversed in the gap. Derive the modulation factor M for a gap across which the electric field varies as

$$E(z) = E,\ 0 \le z < g/2$$

$$= -E,\ g/2 \le z \le g$$

15. Estimate the bunching length for a 500-kV, 300-A pencil beam (i.e., a beam of circular cross section and radius r_b) used in a 1.3-GHz klystron with circular cross section. For this back-of-the-envelope calculation, use the simplified one-dimensional result in Equation 9.11 and ignore any space-charge depression of the beam energy, so that Equation 9.1 holds. Assume the charge density is a constant across the beam. To determine the beam radius, you will need to determine the drift tube radius. For this, choose the cutoff frequency for the TE_{11} mode of the drift tube to be 1 GHz, and maintain a 5-mm standoff between the outside of the solid electron beam and the wall.
16. The perveance of the beam in Problem 15 is $K = 0.85 \times 10^{-6}\ A/V^{3/2} = 0.85\ \mu perv$. Recompute the bunching length as directed in Problem 15 except for a 300-kV beam of the same perveance, 0.85 μperv.
17. Let us examine the low-impedance relativistic klystron of Friedman et al.[23] (a) For a thin annular electron beam of current $I_b = 5.6$ kA and average radius $r_b = 1.75$ cm, accelerated in a 500-kV diode, in a drift tube of radius $r_0 = 2.35$ cm, compute the beam relativistic factor γ_b within the drift tube and the normalized axial velocity $\beta_b = v_b/c$. (b) For that beam, compute the bunching length using Equation 9.15 for a klystron operating at f = 1.328 GHz.
18. Compute the threshold voltage for the unique low-impedance klystron bunching mechanism of Equation 9.18 for the following parameters (see Table 9.6):
    a. 1 MV, 35 kA, $r_b = 6.6$ cm, $r_0 = 7$ cm
    b. 500 kV, 5 kA, $r_b = 2.35$ cm, $r_0 = 2.3$ cm
19. Derive the expression for the quality factor Q given in Equation 9.22 for the cavity in Figure 9.10 in terms of the lumped circuit elements shown there. Find an expression for the frequency at which the cavity impedance of Equation 9.20 drops to half of its peak value as a function of ω_0 and Q.
20. Assume we have a cavity with the following parameters: $f_0 = \omega_0/2\pi = 11.424$ GHz, characteristic impedance $Z_c = R/Q = 27\ \Omega$, and quality factors $Q_b = 230$, $Q_e = 300$, and $Q_c = \infty$ (i.e., we are assuming the cavity walls are perfectly conducting, so that there are no resistive losses in the walls). (a) What is the cavity impedance at f = 11.424 GHz? (b) What is the cavity impedance at f = 11.4 GHz? (c) At what frequencies is the real-valued magnitude of the complex impedance, $|Z|$, equal to half of the value at 11.424 GHz? (d) Assuming the rise time of a microwave signal injected into the cavity is approximately equal to the RC time constant of the cavity (Equation 9.22), estimate the rise time for the injection of an input signal into the cavity.
21. In many klystrons, the designer maximizes power and gain by detuning the penultimate cavity so that its resonant frequency lies above the signal frequency, as indicated in Figure 10.7. This tuning makes the cavity impedance appear to be inductive to the bunches on the beam. This issue is discussed, for example, by Houck et al.[39] Consider the cavity voltage–current relationship of Equation 9.19, with the impedance given in Equation 9.20. Assuming, as in the reference, that the electrons in the leading edge of a bunch are moving faster than those at the trailing edge, show how one adjusts the phase relationship between the voltage and current, through the impedance, in order to slow down the electrons at the front of the bunch and accelerate those at the back.
22. Plot the space-charge-limiting currents for a thin annular beam as a function of wall radius, assuming a 2-mm standoff between wall and beam, for voltages of 1, 1.5, and 2 MV.